Archive of SID

Journal of Applied Fluid Mechanics, Vol. 12, No. 1, pp. 145-154, 2019.
Available online at www.jafmonline.net, ISSN 1735-3572, EISSN 1735-3645.
DOI: 10.29252/jafm.12.01.29179

Experimental and Computational Simulation of an Open Terrain Wind Flow around a Setback Building using Hybrid Turbulence Models

K. B. Rajasekarababu and G. Vinayagamurthy†

Aerodynamics laboratory, School of Mechanical and Building sciences VIT- Chennai. Chennai -600127, India

†*Corresponding Author Email: vinayagamurthy.g@vit.ac.in*

(Received May 8, 2018; accepted August 13, 2018)

ABSTRACT

In recent days, building aerodynamics has gained more attention to urban planners, architects, and wind engineers in understanding the wind flow behaviors around tall buildings. CFD (Computational Fluid Dynamics) simulations are the major tool regularly carried out to assess the wind flow pattern around the buildings to demonstrate the atmospheric and wind tunnel environment in accordance with the turbulence parameters. One of the most challenging tasks is to evaluate a turbulence model which precisely represents atmospheric turbulence flow using computation resources. This study is intended to analyze the precision and numerical stability of open terrain wind flow around a setback building with sharp edges of aspect ratio of 1:5. Hybrid turbulence models using Delayed Detached Eddy Simulation (DDES) and Improved Delayed Detached Eddy Simulation (IDDES) are employed with (Y^+) wall treatment in combination with roughness parameters. From the numerical simulation, the size of re-circulation zones in addition to wake separation zones in a three-dimensional plane are determined to assess the flow characteristics of the building at 0^0 wind incidence. The mean pressure coefficients ($C_{P\ mean}$) are validated against the results obtained from Boundary Layer Wind Tunnel (BLWT) experiments carried out at CSIR-Structural Engineering Research Centre, Chennai.

Keywords: Set-back building; Open-terrain; Wind pressure on the structure; IDDES; DDES.

NOMENCLATURE

ABL	Atmospheric Boundary Layer	PSD	Power Spectral Density
AIJ	Architectural Institute of Japan	RANS	Reynolds Averaged Navier Stokes
C_s	roughness constant (0.5)	RMS	Root Mean Sqaure
D	width of the building.	TKE	Turbulent Kinetic Energy
$C_{P\ mean}$	mean pressure coefficient	U_x	velocity at x-direction
DDES	Delayed Detached Eddy Simulation	U_H	velocity at reference height "H"
DES	Detached Eddy Simulation	WMLES	Wall modeling LES
IDDES	Improved Delayed Detached Eddy Simulation	y	maximum coordinate height
		u^*_{ABL}	atmospheric Boundary layer frictional velocity
F1& F2	shielding functions		
f_B	blending function	y	aerodynamic roughness height
f_d	delay function		
f_e	elevating-function	Cμ	empirical constant (0.09)
GIS	Grid Induced Separation	ε	turbulent dissipation rate
K_s	sand grain roughness	κ	karman constant (0.4)
LES	Large Eddy Simulation	ω	turbulent specific dissipation rate
L_{hybrid}	hybrid length scale	Δ	grid spacing

1. INTRODUCTION

Tall structures are often subjected to wind force such that the interaction of the wind on the structure has to be given special attention for structural engineering and architecture. Numerical simulations have capabilities to generate external environmental flows and predicting surface pressure. Computational simulations of tall buildings are

www.SID.ir

Archive of SID

challenging due to its extreme 3D structure and regularly related with vast extend of flows such as unsteady vortex shedding, strong shear layer and separations. Capturing of flow is a tedious task using the measuring techniques and its accurate modelling is even more difficult. Several researches have been carried out on wind- induced loads on conventional and unconventional tall buildings. In recent trends, aerodynamic modification on tall buildings is investigated to counteract the effect of wind load on tall buildings. Wind-induced load is calculated by pressure coefficients using wind tunnel test and numerical simulations. The study investigated the influence of turbulence on surface pressure field and forces acting on buildings with a different plan. Kareem (1989) investigated the influence of flow in terms of surface pressure on a rectangular prism of 1:1.5 side ratio and 1:5 aspect ratio. Wang, Zhou, Chan, Wong, and Lam (2004) conceptualizes horseshoe vortex, up- stream base vortex and tip vortices formation for a rectangular building. This study provides a good view of general flow features on the conventional tall buildings. Tanaka, *et al.* (2012) presented flow features, pressure coefficients, overturning moment coefficients and PSD by using numerical and experimental results for an aerodynamically modified tall building like a square, corner cut, rectangular, triangular, tilted, tapered, helical and setback models. Kim and Kanda (2013) performed time domain analysis and frequency domain analysis on the square, tapered and set-back models with a side ratio of 1:1. There has emerged a number of researches for exploring the wind flow around unconventional buildings. Chakraborty *et al.* (2014) enumerated the results of a wind-tunnel study and numerical studies on plus (+) plan shaped tall building at different wind incidence angles. Joubert, *et al.*(2015) discussed time-averaging three dimensional flow around a prism using PIV and further validated with computational results. Paul and Dalui (2016) have investigated the surface pressure and wind effects on Z plan shaped building using numerical simulation. Numerical turbulence modeling is challenging to reproduce accurately corresponding to wind tunnel flow or terrain flows. This is due to wide-range turbulent flow effects and complexity of turbulence scales. These scales have no mean flow as it affects specific flow regimes resulting in computational inaccuracies and leading to extensive time. Robustness and simplicity made RANS models to be used widely. It works excellently for attached boundary flows, but it is not suitable for stagnation and separated zones. On another hand, LES (Large Eddy Simulation) is better than RANS, but it requires finer mesh in wall regions to resolve near wall eddy structures and consumes longer time (20 times) to solve the complex turbulence flows compared to RANS model. Meanwhile, the efficiency of RANS & accuracy of LES is amalgamated as DES introduced by Spalart, *et al.* (1997). For highly separated flows, DES is used (combination of RANS & LES) by Spalart-Allmaras with RANS model (single equation model). For a simple modification, DDES is included as a function in classical DES where the model is ”shield” against the grid induced separation defined by Spalart (2006). This modified formulation preserves the RANS model throughout the boundary layer as it uses some blending functions as a key point to define the length scale. DDES identifies boundary layers and preserves the full RANS model even if the grid spacing is limited. The blending function analyzed by Menter, *et al.*(2003) uses internal length scale of the RANS model and the wall distance. These ’shielding’ functions are usually in the boundary layer (F1=1) or at the edge of the boundary layer (F2=0). Another well-improved turbulence model is IDDES where its objectives are to add on the advantages of the WMLES and the DDES efficiency by Shur, Spalart, Strelets, and Travin (2008). This indicates that at inner RANS and the outer LES regions, DES could be developed into a suitable WMLES formulation resulting in IDDES model. IDDES model features have complex blending function allowing to be used in DDES and WMLES mode combined with SST model (Shear Stress Transport). This calibration and combination give more reliable, simple and accurate results. The above methodology has been carried out in a detailed manner for the computational simulation on a setback building. In the present study, pressure distribution obtained from the numerical analysis is validated against wind tunnel experiment and time-averaged velocity profiles around the building are analyzed using numerical simulation.

2. HYBRID TURBULENCE MODEL

The classic DES of Spalart *et al.*(1997) is premature in switching from RANS to LES based on the computed length scale results that under-predict wall stresses or Modeled Stress Depletion (MSD). The hybrid RANS and LES combination turbulence model has ultimate aim for improved accuracy and robustness. The hybrid DDES and IDDES [Spalart *et al*, (2006) and Shur *et al.* (2008) respectively] have used two-equation SST-mentor model Menter *et al.*(1994). DDES model was formulated to avoid MSD in ambiguously-refined grids through the introduction of a shielding function that incorporates the eddy viscosity in determining the switch between the RANS and LES regions. DDES extension component of IDDES, incorporates the benefits of LES inlet conditions (WMLES) and DDES. IDDES model is formulated by improving the destruction term and introducing a length scale, L_{hybrid} in the below given TKE equation.

$$\frac{\partial(\rho k)}{\partial t}+\frac{\partial(\rho u_j k)}{\partial x_j}= \frac{\partial}{\partial x_j}\left(\left(\mu+\frac{\mu_t}{\sigma_k}\right)\frac{\partial k}{\partial x_i}\right)+\tau_{ij}S_{ij}-\frac{\rho k^{3/2}}{L_{hybrid}} \quad (1)$$

For IDDES, the length scale of L_{hybrid} can be written as

$L_{\text{hybrid}}=L_{\text{IDDES}}= f_d(1+f_e)\times L_{\text{RANS}}+(1- f_d)\times L_{\text{LES}}$ where the length scale of L_{RANS} is defined as $k^{0.5}/(\beta^*\omega)$ and L_{LES} is defined as $C_{\text{DES}} \times \Delta$, where $\Delta= \max(\Delta x, \Delta y, \Delta z)$. For IDDES, the grid scale function f_d is defined as max $[(1-f_{dt}); f_B]$. It is determined by both the geometry part f_B and the flow part $(1-f_{dt})$. When f_e is larger than zero and f_d is equal to f_B, $L_{\text{IDDES}}=L_{\text{WMLES}}=f_B\ (1+f_e)\times L_{\text{RANS}}+(1-f_B)\times L_{\text{LES}}$, and it

www.SID.ir

Archive of SID

acts in WMLES mode [Zhixiang Xiao *et al.* (2014)] and is redefined as $\Delta=\min[\max(C_w\Delta_{max}; C_wD_w; \Delta_{min}); \Delta_{max}]$.When f_e is equal to 0, $L_{IDDES}= f_d \times L_{RANS}+(1- f_d)\times L_{LES}$ and it acts in DDES mode.

3. METHODOLOGY

3.1 Set-Up Description

The study focuses on a rectangular setback building model with a full scale height of 210 m. The building is divided into three setbacks and a roof. The building has a side ratio of 1:1.5 and area ratio of the roof–floor to base-floor is 1:6.25. The model scale factor of 1/300 is chosen for experiment and its blockage ratio is 2.3%. The setbacks are so divided such that the longer dimension is 0.015 m on either side of the building at each setbacks and the shorter dimension is 0.010 m at each deck. Thereby setback reduction ratio (longer side: shorter side) of 1.5:1.0 is maintained at all decks. The scaled building model height (H) is 0.7 m with base deck dimension 0.15 m x 0.10 m and the subsequent higher decks with reduced dimensions are 0.12 m x 0.08 m, 0.09 m x 0.06 m and 0.06 m x 0.04 m as shown in Fig.1.

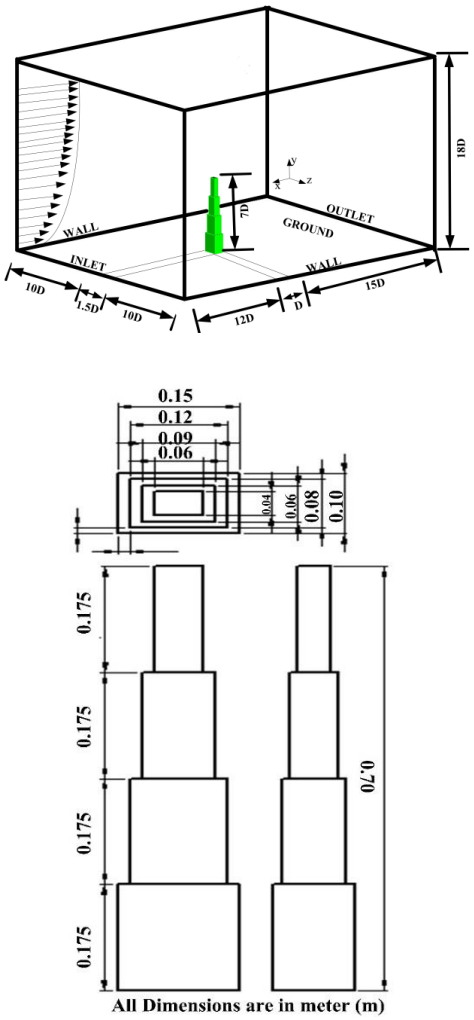


Fig. 1.Conceptual representation of a wind tunnel the domain and Elevation, Plan.

3.2 Wind Tunnel Test

Wind tunnel measurements for the above model are obtained in the open circuit Atmospheric Boundary Layer (ABL) wind tunnel of CSIR-SERC (Council of Scientific and industrial Research-Structural Engineering Research Centre) Chennai, India. The specification of open-circuit ABL wind tunnel test section is 2.5 m x 2 m x 1.8 m and blockage ratio of the model is taken as 2.3 %, which is a permissible value (max 5% from AIJ Guidelines by Tominagaa *et al* (2007). The model is tested at zero angle of incidence and the longer side is taken as the windward. The pressure ports are located at 10 % of the height near each setback deck (y/H = 0.225, 0.475, 0.725, and 0.975). The pressure tubing system used in this investigation is pre-calibrated as per the instruction given in Selvi Rajan *et al.*(2008). The edge ports are made to study the aerodynamic behavior closer to the model. The open terrain ABL profiles are simulated at the mean wind speed of U_H= 13.6 m/s and turbulent intensity is 12%.

3.3 Computational Grid and Domain

The constructed computational domain exactly resembles the wind-tunnel test section. Computational domain has been deployed with ABL profile and this ensures fully developed flow which follows the best-practice guidelines of Franke *et al.*(2007). The computational grid is a fully structured hexagonal having a stretching ratio of 1.12 and cell height 0.0020 m at the wall. The results of grid sensitivity analysis are presented in Fig.2 b. To improve the results and capture the small eddies around the building, a grid adaption is made around the building. The adaptive mesh region comprises of the upstream 2D, downstream 7D, and the sidewall 1D regions as shown in Fig.2 b. Jianlin and JianleiNiu (2015) used DES on environmental flows and thermal comfort around an isolated building with low number of mesh and low computational time. The technique demonstrated that the flow field is similar to LES.

Boundary conditions

At inlet of the domain, the approached flow is imposed based on wind tunnel measurements (wind speed of vertical profile and turbulence). The profiles are defined according to the logarithmic law given by Eq. (2), where $y_0$is roughness height of the ABL and u^* is shear velocity.

$$(U_y)=\frac{u^*_{ABL}}{\kappa}\ln\left(\frac{y+y_0}{y_0}\right) \tag{2}$$

with κ being the Karman constant (0.4) and y being the coordinate height.

$$\varepsilon(y)=\left(\frac{(u^*)^3}{\kappa(y+y_0)}\right) \tag{3}$$

$$\omega(y)=\left(\frac{\varepsilon(y)}{C_\mu k(y)}\right) \tag{4}$$

The turbulence dissipation rate *(ε)* is given by Eq. (3) and the specific dissipation rate *(ω)* is given by Eq.

www.SID.ir

Archive of SID

(4) where C_μ is an empirical constant (0.09). Wall functions of Launder and Spalding (1974) with roughness modification of Cebeci and Bradshaw (1977) are used for ground surface. The sand grain roughness height of K_s = 0.0019 m and the roughness constant of C_s = 0.5 are used. These relationships are based on derivation of aerodynamic roughness length (y_o) equation from Blocken, Stathopoulos, and Carmeliet (2007) as shown in Eq. (5). In the simulation, the value of sand grain surface of a building is considered as zero (K_s=0).

$$K_s = \frac{9.793 y_0}{C_s} \tag{5}$$

Zero static pressure is applied at the outlet of the domain whereas, the inlet of the computational domain is imposed with open terrain atmospherics wind and turbulent properties. The top and side walls of the domain are applied with wall type boundary conditions.

2.5 Solver Settings

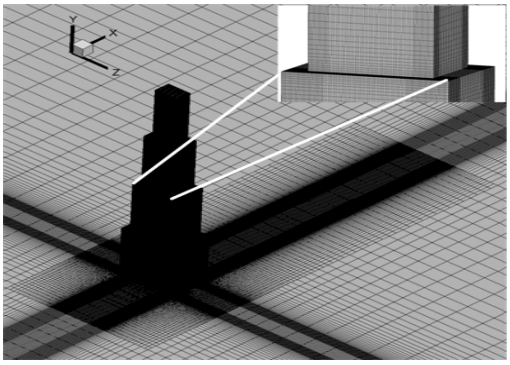
The simulations were performed using ANSYS FLUENT 16, where SIMPLE (Semi-Implicit Method for Pressure-Linked Equations) was used as the pressure-velocity coupling algorithm. 3-D unsteady Reynolds- Averaged Navier-Stokes equation is used to solve in DDES and IDDES combination with Shear Stress Transport (SST). In spatial discretization, Least Square Method Cell-Based gradient and second-order upwind schemes were used for solving pressure, momentum, turbulent kinetic energy, and turbulent dissipation. The convergence will be acquired when all the scaled residuals are leveled off and achieved at least 10^{-6} for XYZ momentum and K, ω and continuity. The assumed residuals of the computational simulation were achieved and were monitored over a time period of 1.2 s approximately.

3. RESULTS

A grid independence test was done by comparing results of the three grids namely coarse, medium and fine. The fine computational grid is shown in Fig. 2a and the number of elements are shown in Table 1. In order to reduce computational time and discretization error, grid independence analysis is highly significant. The test was limited to sand grain roughness height (K_s < Y+). The mean pressure coefficient of a building surface at the height y/H=0.225 is taken and compared with experimental results. Both turbulence models show good results for fine mesh and is shown in Fig. 2b. Upstream mean wind velocity profile as per wind tunnel flow has been investigated and compared with two turbulence models (DDES and IDDES). Fig. 2b describes mean velocity profile corresponding to wind tunnel experiment along with computational simulation.

Table 1 Grid independence and grid size

Name	Δ_x	No. elements
Coarse	0.0025	2759640
Medium	0.0020	3657335
Fine	0.0020	8872488



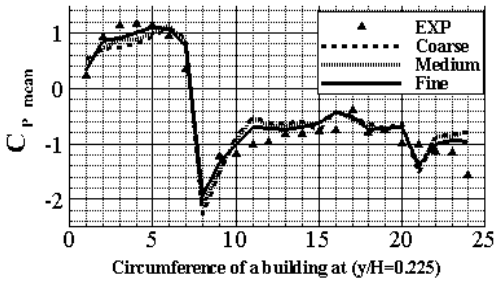


Fig. 2.a Grid sensitivity comparison using Cp mean at y/h=0.225.

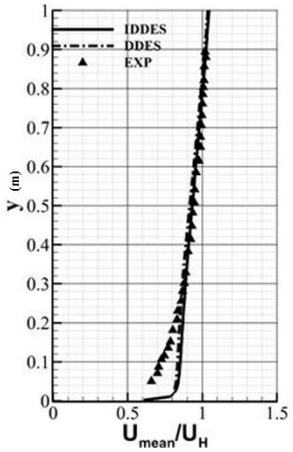


Fig. 2.b Inlet velocity profiles.

3.1 Flow Phenomenon

The U_x/U_{mean} profiles at 4 different levels near the edge of the building (y/H=0.225, y/H=0.475, y/H=0.725 and y/H=0.975) were compared with DDES and IDDES turbulence models in order to validate the simulation results. In Fig. 3, the upstream stagnation and downstream recirculation data are compared. The numerical accuracy was determined by the same results reproduced by the two models at upstream stagnation (a to d). The stagnation effects are visible at different heights y/H=0.225, y/H=0.475, y/H=0.725 and y/H=0.975 with velocities varying along the building height gradually due to boundary layer shown in Fig.3. Height, y/H =0.225 depicts standing and base vortex due to strong no-slip condition and downdraft near the base of the building. This proves that ground roughness and scooping effect (upstream flows down the wind ward and as a result the air collects from the higher levels to the ground level) dominates at base

www.SID.ir

Archive of SID

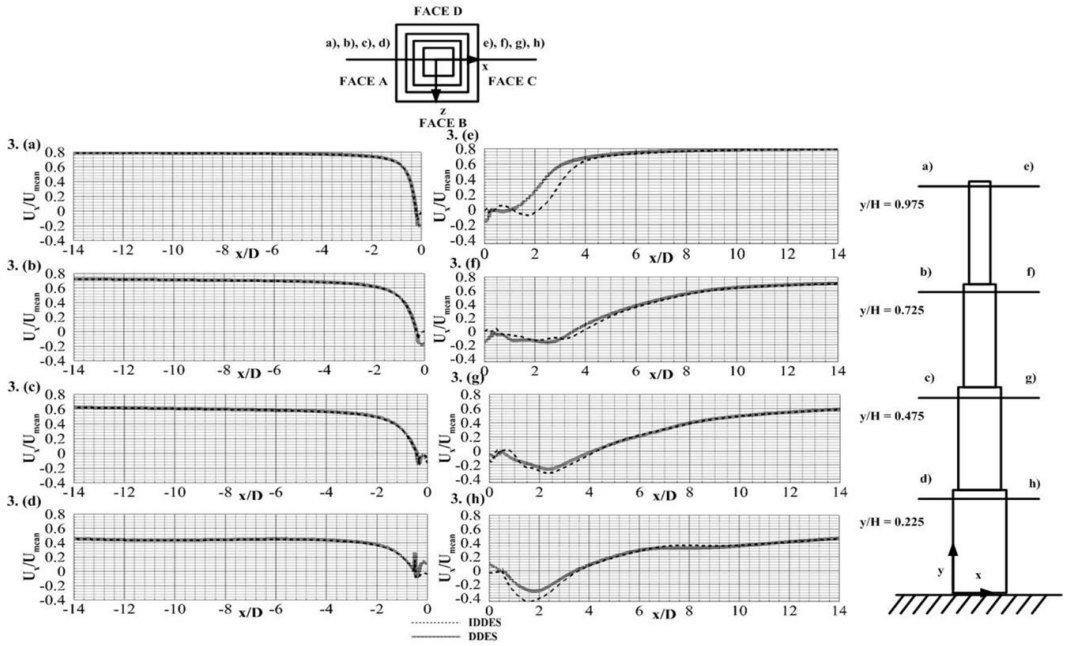


Fig. 3. Time – averaged velocity profile on stagnation upstream region (a – d) and downstream recirculation zone (e – h) for various decks (levels).

of the building. At downstream, some deviations are measured in re-circulation zones as shown in Fig. 3 [e) to h)]. The DDES under predicts the tip vortices and base vortices compared to IDDES at heights y/H=0.225 and y/H=0.975. At the downstream, almost near 4D, DDES under predicts the re-circulation and flow magnitude.

3.2 Mean and RMS Wind Pressure Coefficients

To analyze the surface pressure distribution over a setback building, it is necessary to validate and verify the correctness of computational simulation and accuracy of turbulence models. Ben Mount*ed al.* (2017) computationally investigated the effect of dimensional variation of pressure coefficients in rectangular buildings. They conducted benchmark study on CAARC building model to validate the simulation accuracy. Following it, this investigation validates both accuracy and efficiency of this CFD simulation. The experimental $C_{P\ mean}$ and $C_{P\ rms}$ pressure values are validated with CFD simulations using two hybrid turbulence models. The wind pressure coefficients on surface of the setback building were converted to non-dimensional quantity by Eq. (6).

$$C_{Pmean} = \frac{p - p_0}{\frac{1}{2}\rho U_H^2} \tag{6}$$

where p is the pressure extracted from the target point, p_0 is the reference pressure at the height of point p, ρ is the density of air (1.225 kg/m^3) and U_H is the mean wind velocity at height H. The distributions of the mean pressure coefficient for four different levels (y/H=0.225, y/H=0.475, y/H=0.725 & y/H=0.975) are extracted. In Fig. 4 (a), the mean pressure coefficients of DDES and IDDES turbulence models coincide with those wind tunnel experimental results. Mean pressure coefficient distribution shows positive values of C_P on windward face. At height y/h=0.225, graph depicted a peak negative pressure coefficient (nearly 1.8) which indicates a high suction due to sharp edges and corner effects. At heights y/H=0.475 and y/H=0.725, $C_{P\ mean}$ shows a good arrangement with experimental results. At the roof of the building (y/H=0.975), $C_{P\ mean}$ shows dispersion with experimental values due to strong corner effect resulting due to the acceleration of flow. Compared to experimental result at the height y/H=0.975, the CFD simulation under predicts the $C_{P\ mean}$ due to the 3D tip vortices produced over the roof as a result of the expansion of vortices.

Fig.4 (b) compares the $C_{P\ rms}$ (root mean square) values on circumference of setback building at the height of y/H=0.225 obtained from IDDES turbulence model and wind tunnel experiment respectively. The IDDES $C_{P\ mean}$ values showed good agreement with experimental results whereas, variations were observed on the $C_{P\ rms}$. The maximum deviation found at leeward nearly 19% from experimental values.

3.3 Time Averaged Velocity Profiles and Side Wall Re-Circulation

The side wall velocity profiles of DDES and IDDES turbulence models are compared in Fig. 5. Both turbulence models performed identically in side wall regions, particularly in the tip of upstream and edge of downstream of the setback building. But most significant velocity fluctuation is found in mid-width of the building. In the mid width of the building, profile starts from zero and extends forth and back

www.SID.ir

Archive of SID

due to velocity gradient at the downstream where the velocity profile extends outward perpendicular to the flow due to viscous stress at all the decks. Although the downstream edge recirculation zone is close to zero in all regions and the velocity changes accordingly from the lower level to higher level, some deviations were found largely at the bottom of two decks because of strong slip-stream. This has resulted the velocity profile to fluctuate at the mid-width of side wall.

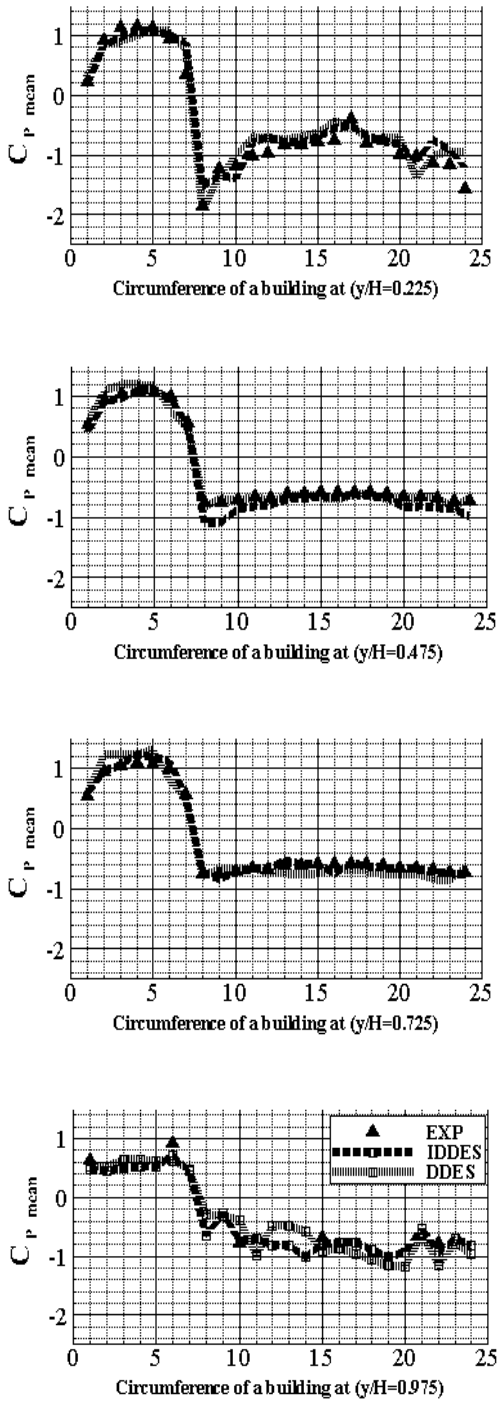


Fig. 4 (a) Mean coefficient of pressure at different height of a setback building.

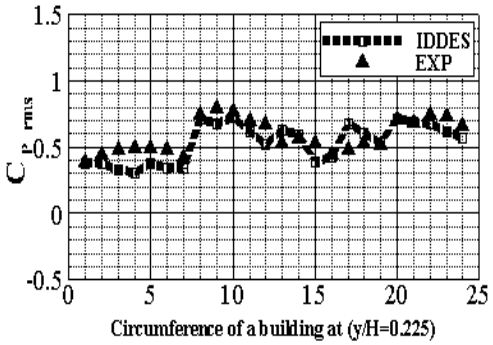


Fig. 4 (b) RMS pressure coefficient at different height of a setback building.

3.4 Time Averaged Horizontal and Vertical Wake Velocity Profiles

Wake recirculation measurement is a difficult task. In this simulation, the results for both turbulence models for the mean velocity component at different heights are compared accordingly. The wake recirculation region around a building is quantified with a width (D) of the building. In this case, results are processed at edges of the deck (vertical cross section) making possible to measure the recirculation length at each height and interpolate between them Fig.6 (a). The vertical flow around the building in Fig. 6 (b) shows strong upward movement at y/H=0.475 and 0.225 which indicates maximum wake (0.20 U_{mean}) occurring at the distance of nearly 3D from the building. The downward movement is dispersed at a height of y/H=0.725 due to strong downward flow movement which is visible with a maximum wake (0.20 U_{mean}) at the distance of nearly 2.5D from the height of 3rd and 4th levels (y/H = 0.725, 0.975).

Considering the side wall recirculation velocity profiles in Fig. 7a, it can be seen that the flow tends to move upward in the top two decks and the lower deck. Due to the existence of vortex, large velocity gradient makes the flow move downwards. The down draft was further verified using the measured pressure values from the wind tunnel experiment where the pressure was found to be acting on the surface, giving rise to a positive pressure. The upward flow i.e. y/H=0.975 has the maximum value of 0.2U at the distance of 0.4D from the building. Near the base, the levels corresponding to y/H=0.225 and y/H=0.475, the down flow is observed to have a magnitude of 0.2U at a distance of y/H=0.475.

The horizontal component of flow in Fig.7b shows a strong movement away from the building at the height of y/H=0.225 and y/H=0.475 with the magnitude of 0.5U at a distance of 0.8D from the building side wall. The direction of flow is inversed due to the presence of base vortex. At the height of y/H=0.725 and y/H=0.975, it shows the setbacks on the tall building reduces the horizontal movement along with height.

www.SID.ir

Archive of SID

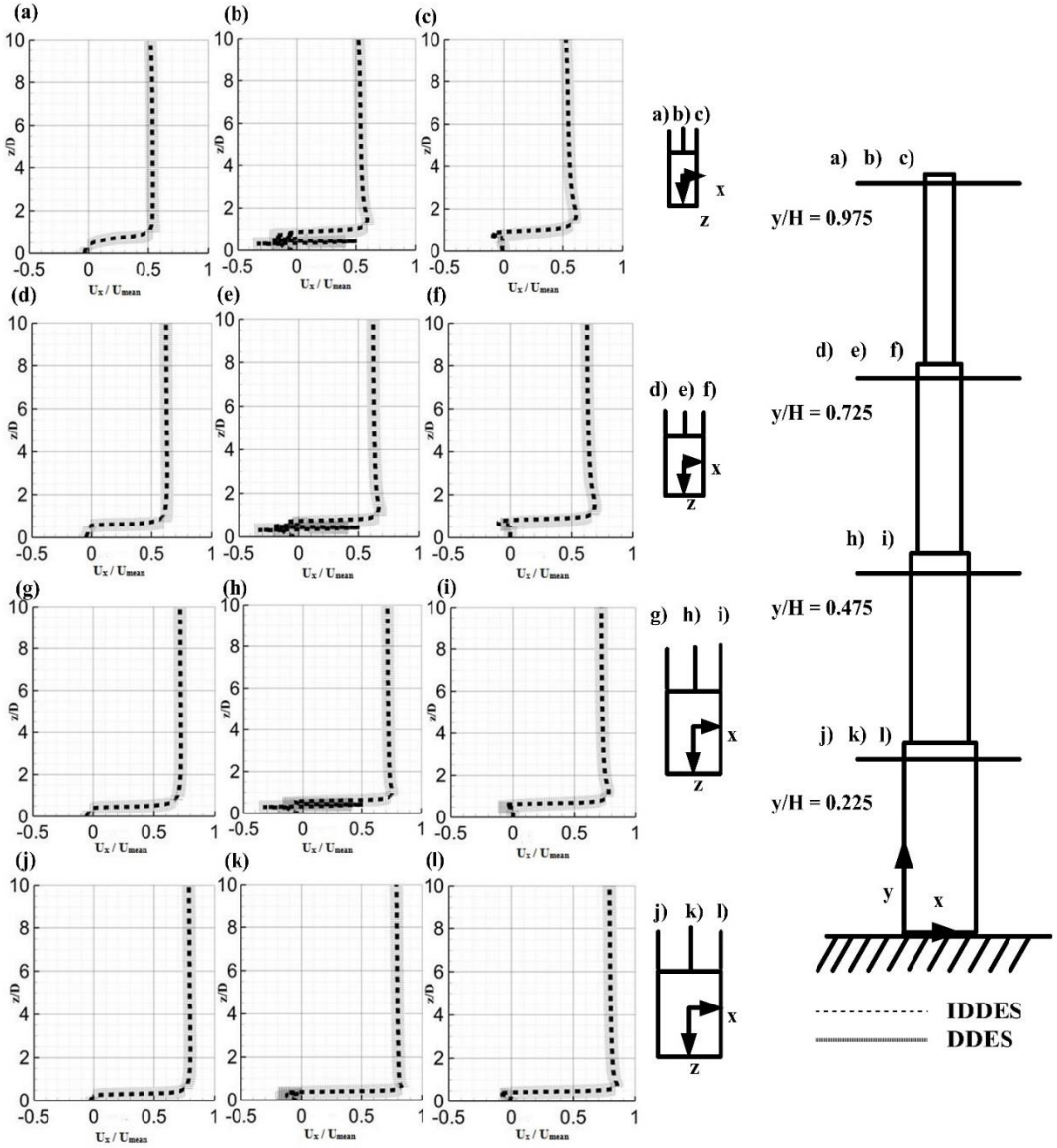


Fig. 5. Time - averaged velocity profiles for side-wall recirculation.

3.5 Time Averaged Vortex Structure in the Wake of Hybrid Turbulence Models

The vortex formations on setback building are compared with the hybrid turbulence models. To visualize the vortex structures behind the setback building, a Q-criterion were used which identifies the wake vortices. The Q- criterion is defined as in Eq. (7).

$$Q = \frac{1}{2}\left(r_{ij}r_{ij} - s_{ij}s_{ij}\right)$$
$$s_{ij} = \frac{1}{2}\left(\frac{\partial u_i}{\partial x_j} + \frac{\partial u_j}{\partial x_i}\right), r_{ij} = \frac{1}{2}\left(\frac{\partial u_i}{\partial x_j} + \frac{\partial u_j}{\partial x_i}\right) \quad (7)$$

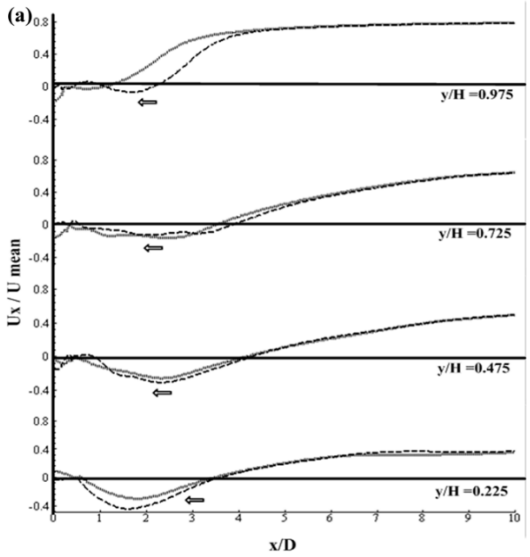
The Q value was chosen as 1500 in this study, in order to obtain preferred flow structure and however to exclude small-scale vortices which were of no interest. The time-averaged vortex structures identified by Q=1500 behind the building with DDES and IDDES turbulence models using fine mesh are shown in Fig.8. It represents the capability of the simulation to solve turbulence with provided shielding function for SST-based DDES and IDDES model to achieve high chaotic large and small scale vortices. Both DDES and IDDES capture the massively separated flow of 3D stream wise and transverse vertical structures. At the same time, it reveals some differences especially in the side separation region and wake region. The DDES model has captured most of the large vortex structure in wake zone. The IDDES model shows the large vortices which extends with shedding of vortices. The IDDES turbulence model captures wake expansion and base trailing vortices.

4. Summary and Conclusions

In this investigation, DDES and IDDES turbulence models were selected to analyze the atmospheric wind flow around a tall setback

www.SID.ir

Archive of SID



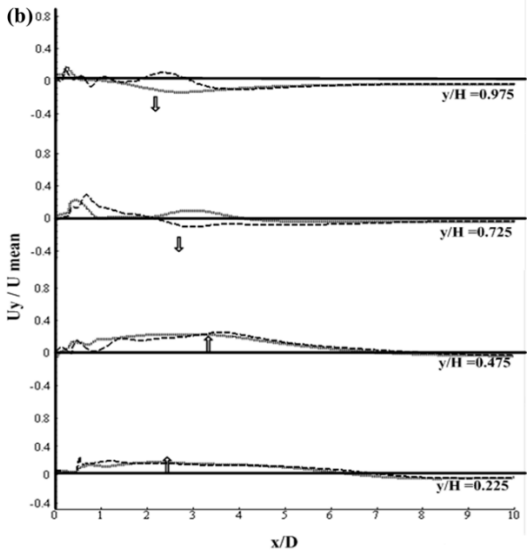
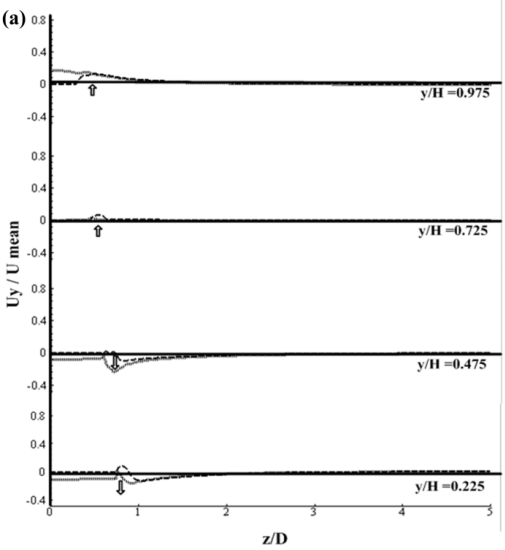


Fig. 6. Time averaged Horizontal velocity profile in the wake for u_x and u_y a) Horizontal velocity and b) Vertical velocity.



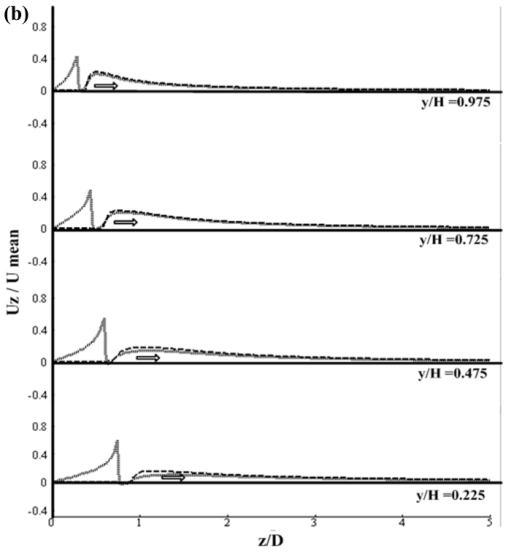


Fig. 7. Time averaged Horizontal velocity profile on side wall region for u_y and u_z a) Vertical velocity and b) Horizontal velocity.

building. The experimental data is obtained through PSI scanner in the form of time varying wind pressure from each port. In computational simulation, DES modified SST, DDES and IDDES turbulence models are applied to a complex unsteady flow in the combination of roughness (sand grain) wall treatment with open terrain atmospheric inlet boundary conditions. Experimental and simulation $C_{P\ mean}$ values were compared to determine the accuracy of the simulation results. Both DDES and IDDES performed well in the near wall regions but some errors were found at the roof (y/H=0.975). Mean *Cp* values are positive on the windward and negative on the other sides of the building leading to huge suction. The DDES turbulence models under predicted the suction pressure. This validation study computationally validates wake recirculation zones on setback buildings. The flow fields are measured at 10 % of the height near each setback deck (y/H=0.225, 0.475, 0.725 and 0.975). The assessed upstream and downstream flow fields are made to study the effects of turbulence model at setbacks. The comparison of computational simulation results shows that the DDES and IDDES qualitatively reproduce the upstream flow features of the building. Furthermore, it shows a dispersion occurring in downstream recirculation zone. In mid-width of the building, the side wall recirculation zone wake extends outward and inward perpendicular to the flow and reduces throughout the height due to wake vortices. In wake regions, the iso-surface shows the vortex structure in which IDDES captures trailing vortex and DDES captures the arc vortex. Overall,

www.SID.ir

Archive of SID

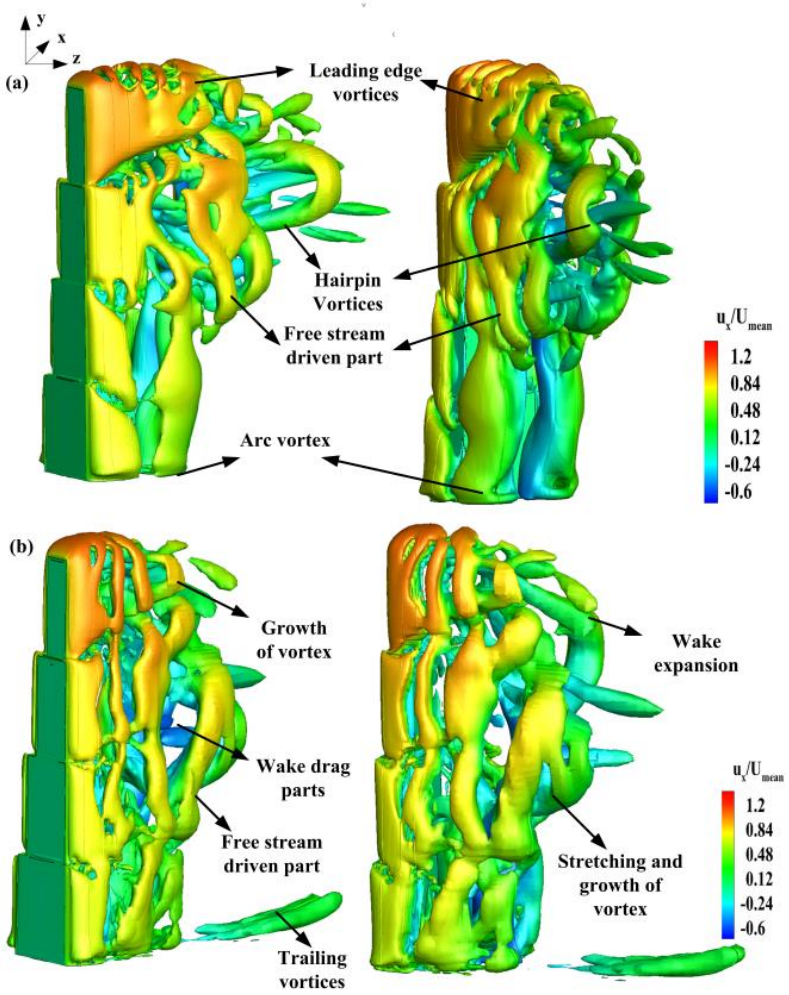


Fig. 8 a) DDES b) IDDES Iso-surface (Q=1500).

from the two turbulence models, IDDES produced $C_{P\ mean}$ similar to experimental results. This turbulence model is possible to quantify the complex flow in detail with limited grid spacing but due to computational necessity it is not realizable with more complex LES. The extremely complex flow around setback building can be better understood using the above results.

ACKNOWLEDGEMENTS

We sincerely express our thanks to Director and Staffs of CSIR- SERC Wind engineering laboratory, Chennai and Aerodynamics laboratory VIT-University Chennai for their unconditional support in conducting experiments at BLWT and computational facility.

REFERENCES

Blocken, B., T. Stathopoulos and J. Carmeliet (2007). CFD simulation of the atmospheric boundary layer: wall function problems. *J. Atmos Environ*.

Cebeci, T. and P. Bradshaw (1977). Momentum transfer in boundary layers. *Hemisphere Publishing Corp*. New York:

Chakraborty, S., S.K. Dalui and A.K. Ahuja (2014). Wind load on irregular plan shaped tall building—a case study. *Wind Struct 18*(6), 59–73

Franke, J., A. Hellsten, H. Schlünzen and B. Carissimo (2007). Best practice guideline for the CFD simulation of flows in the urban environment. Brussels. *COST Office*.

Joubert, E. C., Harms, T. M., & Venter, G. (2015). Computational simulation of the turbulent flow around a surface mounted rectangular prism. *Journal of Wind Engineering and Industrial Aerodynamics* 142, 173-187.

Kareem, A. (1989). Mapping and synthesis of random pressure fields. *Journal of Engineering Mechanics* 115(10), 2325-2332.

Kim, Y. C. and J. Kanda (2013). Wind pressures on tapered and set-back tall buildings. Journal of Fluids and Structures 39, 306-321.

Launder, B. E. and D. B. Spalding (1974). The computation of turbulent ows. Comp Meth

www.SID.ir

Archive of SID

Appl Mech Eng 3, 26989.

Liu, J. and J. Niu (2016). CFD simulation of the wind environment around an isolated high-rise building: An evaluation of SRANS, LES and DES models. *Building And Environment* 96, 91-106.

Menter, F. R. (1994). Two-equation eddy-viscosity turbulence models for engineering applications. *AIAA Journal* 32(8), 1598-1605.

Menter, F.R., M. Kuntz and R. Langtry (2003). Ten years of experience with the SST turbulence model. *4th International Symposium on Turbulence Heat and Mass Transfer* 625–632

Mou, B., B. J. He, D. X. Zhao and & K. W. Chau (2017). Numerical simulation of the effects of building dimensional variation on wind pressure distribution. *Engineering Applications of Computational Fluid Mechanics 11*(1), 293-309

Rajdip, P. and S. Kumar Dalui (2016). Wind effects on 'Z' plan-shaped tall building: a case study. *Int J Adv. Struct. Eng.* 8*(2016)*,319–335

Selvi Rajan. S, N. Lakshmanan, S.Arunachalam, M. Hannah Angelin and S. Krishnakumar. (2008) Development of a dynamic calibration model for wind tunnel studies *Journal of instrumentation Society of India.* 38, 190-197

Shur, M., P. Spalart, M. Strelets and A. Travin (2008). A hybrid RANS-LES approach with Delayed DES and wall-modelled LES capabilities. *Int. J. Heat Fluid Flow* 29(6), 1638–1649

Spalart, P. R., Deck, S., Shur, M. L., Squires, K. D., Strelets, M. K., & Travin, A. (2006). A new version of detached-eddy simulation, resistant to ambiguous grid densities. *Theoretical and computational fluid dynamics* 20(3), 181.

Spalart, P.R., W.H. Jou and M. Srelets (1997). Comments on the feasibility of LES for wings, and on a hybrid RANS/LES approach. *International Conference on DNS/LES*. USA.

Tanaka, H., Tamura, Y., Ohtake, K., Nakai, M., & Kim, Y. C. (2012). Experimental investigation of aerodynamic forces and wind pressures acting on tall buildings with various unconventional configurations. *Journal of Wind Engineering and Industrial Aerodynamics* 107, 179-191.

Tominaga, Y., Mochida, A., Yoshie, R., Kataoka, H., Nozu, T., Yoshikawa, M., & Shirasawa, T. (2008). AIJ guidelines for practical applications of CFD to pedestrian wind environment around buildings. *Journal of wind engineering and industrial aerodynamics* 96(10-11), 1749-1761.

Wang, H.F. (2004). Flow Structure around a finite-length Square Prism. *Australasian Fluid Mechanics Conference*, University of Sydney

www.SID.ir